ICNTC-2019 Special Issue

J. Indian Chem. Soc.,
Vol. 96, September 2019, pp. 1205-1209

Preparation and characterization of bismuth oxychloride nanoparticles for the development of photocatalytic performance

Bilal İbrahim Dan-Iya and G. Selda Pozan Soylu*

Faculty of Engineering, Department of Chemical Engineering, Istanbul University-Cerrahpaşa, Avcilar, Istanbul, Turkey

E-mail: gpozan@istanbul.edu.tr

Manuscript received online 26 April 2019, revised and accepted 20 July 2019

Bismuth oxychloride nanocomposite was successfully synthesized using bismuth(III) triacetate [$Bi(CH_3COO)_3$] and tin(II) chloride dihydrate ($SnCl_2.2H_2O$) as starting materials. Tetragonal structure and size were characterized by X-ray diffraction whereas SEM shows morphology and dispersion at different magnifications as well as FT-IR spectrum range of 450–4000 cm^{-1} describes the stretching absorption at different absorption bands. The photocatalytic activity of the BiOCl was evaluated by degradation of Bisphenol A (BPA, 2,2-bis(4-hydroxyphenyl)propane). The BiOCl showed a total degradation 100% of BPA in 60 min.

Keywords: Bismuth oxychloride, nanocomposite, sol-gel, photodegradation, BPA.

Introduction

Bismuth oxychloride (BiOCl) is an important nanocomposite material, which has various applications in make-up pigments, batteries, pharmaceutical industry[1,2], photocatalysis[3], optoelectronic and photovoltaic materials acting as lighting diodes, lasers, solar cells, degradation of organic pollutants[4], CO_2 photo reduction, and many more[5]. It belongs to the families of V-VI-VII possessing a wide indirect band gap (E_g = 3.46 eV) and exhibits a p-type semiconducting property[6,7].

As a tetragonal PbFCl structured material, BiOCl crystallizes into peculiar layered structures containing sheets stacked to each other by nonbonding interactions via Cl atoms present in the structure lengthways the c-axis[7]. There exist strong intralayer interactions between bonds and weak interlayer van der Waals forces which in turn give it its tremendous applications ability mentioned earlier[8]. BiOCl possesses an outstanding photocatalytic, photoelectrochemical, optical and electrical properties[6,7]. As a result of its wide application potentials, new economically suitable and simple methods are of paramount importance in obtaining bismuth oxychloride.

Different methods have been used to obtain BiOCl, however, wet chemical method was prominently used in most findings[6,7]. Other procedures include solvothermal[9], chemical vapour deposition[10], sol-gel method, combustion[11], simple hydrolysis[12], ball milling[13], one-step alcohol-heating[14] and many more. Similarly, reported for synthesized nanodisk[15], microspheres[16], nanoflakes[17], nanoplates[18], microflowers[19] and nanosheets[20].

This work presents a simple and economically less costly method of BiOCl nanocomposite synthesis and explaines the photocatalytic activity of BiOCl under UV irradiation.

Experimental

Materials:

Bismuth(III) triacetate [$Bi(CH_3COO)_3$] purchased from Alfa Aesar GmbH & Co KG and Merck 98–101% tin(II) chloride dihydrate ($SnCl_2.2H_2O$, M = 225.63 g/mol) were used as precursors. Ethanol and acetone were used as solvent and additive respectively. Bisphenol A ≥99% purchased from Sigma Aldrich.

Synthesis:

Synthesis of BiOCl nanocomposite was first started by preparing 9 mmol solution of bismuth triacetate [$Bi(CH_3COO)_3$] in 17.5 mL ethanol. Another solution of 4.5

mmol tin(II) chloride dihydrate ($SnCl_2.2H_2O$) was prepared which was added to the 9 mmol solution of bismuth(III) triacetate, followed by addition of 6 mL acetone to the overall mixture. The mixture was stirred for 5 h and aged for 24 h (1 day) at 90°C and calcinated at 500°C for 2 h.

Characterization:

XRD crystal structure of BiOCl was obtained by a Rigaku D/Max-2200 diffractometer, and crystalline size estimated using the Debye-Scherrer formula as follows:

$$D = \frac{C\lambda}{\beta \cos \theta}$$

where C, λ, β, θ are the constant usually with a value of 0.9 or 1, the X-ray wavelength of radiation used (Cu/Kα = 1.54056 Å), the full width at half maximum (FWHM) of diffraction peak and the Bragg diffraction angle, respectively. The spacing *d,* value was also calculated using Bragg's equation.

$n\lambda = 2 \sin(\theta)$

where *'n'* is a numeric constant known as the order of the diffracted beam, λ is the wavelength of the beam, *'d'* denotes the distance between lattice planes, and λ represents the angle of the diffracted wave. The conditions given by this equation must be fulfilled if diffraction is to occur.

Morphology and size distribution of the photocatalysts were documented by scanning electron microscopy (JEOL/JSM-6335F). FTIR analysis was also obtained by Cary 500 UV-Vis spectrometer at room temperature in the range of 450–4000 cm^{-1}. UV-Visible (UV-Vis) DRS was performed using a UV-Vis spectrophotometer (Shimadzu UV 3600), with $BaSO_4$ as the reference.

Photocatalytic measurement:

The photocatalytic activities of the as-prepared samples were evaluated by the decomposition of Bisphenol A (BPA) under UV-Vis and visible light irradiation at the natural pH value and room temperature. In every photocatalytic experiment, 100 mg of catalyst was typically dispersed in 50 mL BPA solution of initial concentration of 25 mg L^{-1} under magnetic stirring.

BPA photodegradation runs were executed with a three-necked quartz batch flask of cylindrical shape. LUZCHEM LZC-5 photoreactor was used in all experiments. The light irradiation were used 16 W and 64 W UV-B lamps (LUZCHEM LZC-UVB). The spectral irradiance of the UV lamp is from 303 to 578 nm and the illumination distance is 18 cm from the target. The light intensity of UV lamp used for degradation experiments was recorded with a visible power meter (Smart Sensor – AR823).

Before the irradiation experiments, the solution was stirred for 60 min in dark to ensure good adsorption equilibrium between the catalyst and the solution. During the irradiation for 60 min, the BPA solution was taken at certain intervals and filtered by means of a PTFE filter (pore size 0.45 μm).

The concentration of BPA and products were analysed by HPLC equipped with C-18 column. The mobile phase used in HPLC consisted of a mixture of acetonitrile/water (60/40, v/v) and was fed into the column at a flow rate of 1 mL min^{-1}.

Results and discussion

Characterization:

The specific BET surface area of the pure BiOCl sample calcined at 500°C is 51 $m^2 g^{-1}$.

Fig. 1 illustrates the XRD pattern of synthesized bismuth oxychloride (BiOCl) nanocomposite.

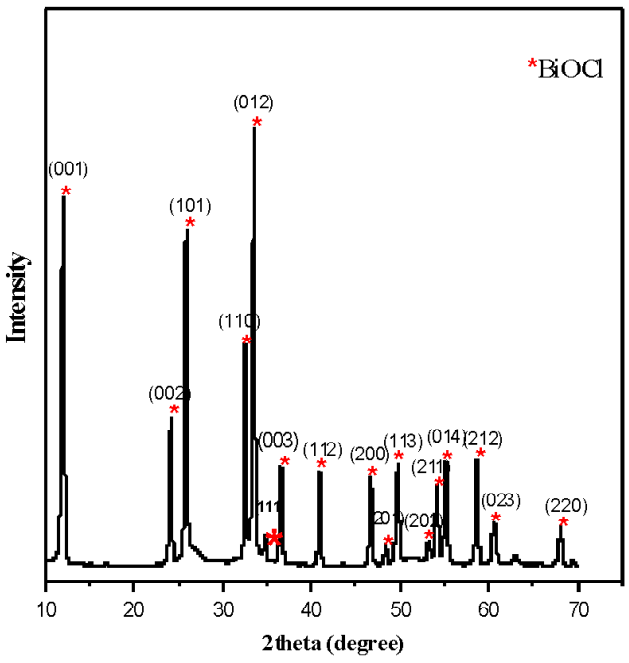

Fig. 1. XRD the XRD pattern of synthesized bismuth oxychloride.

All peaks from the XRD data were confirmed to be representing a tetragonal phase of BiOCl intensity and were in

agreement with the work done by Ascencio-Aguirre[1] in which the tetragonal BiOCl with JCPDS: 96-901-1783 have lattice parameters of a = 3.8861±0.0021 and c = 7.3782±0.0042 in Å units. In this work, peak at 2θ value of 33.5 is the most intensified peak (100% intensity) and as such the calculated crystallite size of the BiOCl with JCPDS file number 01-065-0861 and cell parameters a = 3.8870 Å and c = 7.3540 Å was found to be 37.6 nm. The spacing d, value of the main BiOCl peak was 2.6741 Å.

In addition, Fig. 2 shows the SEM morphologies of BiOCl product with different magnifications. SEM analysis however, exhibits flat and circular sheet-shaped structure in some particles. Thus, there exist some smaller particles which could be other negligible oxides. The morphology of the BiOCl sheets is in relation and similar to the BiOCl sheets synthesized in previous work[9].

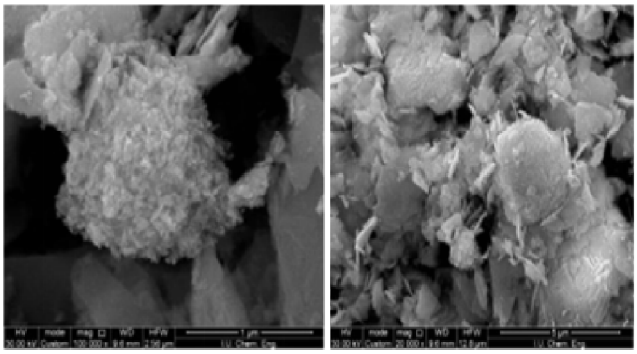

Fig. 2. SEM image of bismuth oxychloride.

FTIR spectrum in Fig. 3 is in the 450–4000 cm^{-1} region. Infrared spectroscopy technology is used to detect the presence of functional groups such as hydroxyl radical (•OH) adsorbed on the surface of synthesized nanoparticles.

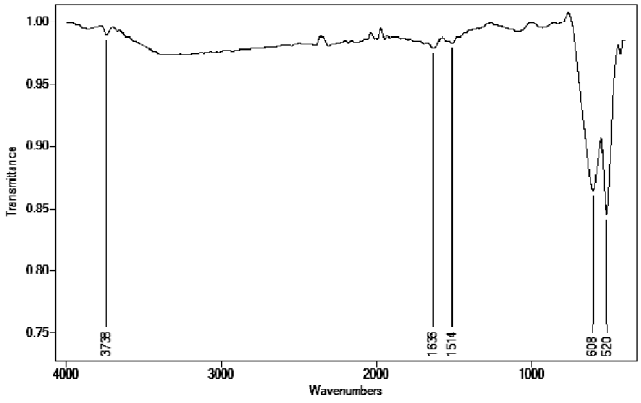

Fig. 3. FTIR spectrum of bismuth oxychloride.

In the photocatalytic degradation experiments, the surface OH groups can not only embrace the photogenerated holes to form hydroxyl radical (•OH) but also serve as active sites for the adsorption of reactants[21]. The weak bands showing in the range of 3200–3800 cm^{-1} with the absorption peak at 3738 cm^{-1} are assigned to the H-O-H stretching from water. The weak bands at 1636 cm^{-1} and 1514 cm^{-1} are due to adsorbed atmospheric CO_2 which results from the preparation and processing of FTIR sample in the ambient atmosphere and the band at 608 cm^{-1} and 520 cm^{-1} are assigned to Bi-O bands, and this was in absolute conformity with work of Li[7].

UV-Vis diffuse reflectance spectroscope (DRS) was used to determine the light absorption characteristics of the prepared binary compounds. For pure BiOCl, the optical band gap width E_g is about 3.3 eV within the UV region.

Photocatalytic activity:

In this study, BPA was preferred as the model contaminat.

BPA, is an organic synthetic compound and a colourless solid that is soluble in organic solvents, but slightly soluble in water. It has been extensively used in the manufacturing of consumer goods and products, such as the monomer for the production of polycarbonate plastics, food and drink packaging materials, protective coatings on metal equipment since first commercial using in 1957[22].

There is an increasing interest in effective remediation technologies to remove BPA from contaminated waters because of being reported to cause not only strongly estrogenic endocrine disrupting effect but also toxicological risk.

In order to detoxify the BPA, various methods have been developed, such as physical adsorption[23], chemical oxidation[24] and biological treatments[25]. Among these methods, photocatalytic oxidation is attracting the widespread attention because of its high activity, high mineralization efficiency, and low toxicity and cost. Oxide-based semiconductors (i.e. TiO_2, Bi_2O_3) in the photocatalytic degradation of the contaminants have been considerably used for decades. However, two main shortcomings impede the practical application of TiO_2 for the pollution control: the large bandgap energy and its poor quantum efficiency. Thus, the development

and executing of new photocatalysts with high light utilization is a necessary.

In this study, the catalytic activity for photocatalytic degradation of BPA over prepared BiOCl was investigated in the presence of a trace of hydrogen peroxide under the optimized conditions. Under the illumination with light source, BiOCl can be excited to generate holes and electrons (eq. (A.1)), and the excited electrons are further transferred to oxygen to form hydroxyl radicals (eq. (A.2)) as described below:

Under the illumination with light source, BiOCl can be excited to generate holes and electrons (eq. (1)), and the excited electrons are further transferred to oxygen to form hydroxyl radicals (eq. (2)) as described below;

$$BiOCl + h\upsilon \rightarrow e^- + h^+ \quad (A.1)$$

$$O_2 + e^- \rightarrow O_2^{\bullet -} \quad (A.2)$$

$$O_2^{\bullet -} + 2H^+ \rightarrow 2^{\bullet}OH \quad (A.3)$$

BPA in the reaction solution is then attacked by the hydroxyl radicals to be oxidized (eq. (3)).

The effect of different UV-B light irridation (16 W and 64 W) on the photo-degradation of BPA over BiOCl catalyst was studied. Under 64 W UV-B illuminations, BPA was more effectively degraded to its by-product and carboxylic acids. It is clearly seen that the degradation of BPA could achieve 70% in 60 min, while only %65 conversion reached under 16 W UV-B illumination.

Moreover, we also studied in various process to determine the effects of adsorption (without the light exposure) with addition of H_2O_2, photolysis under UV-B light (no catalyst) and the degradation of BPA in the absence of H_2O_2 on the photocatalytic activity of BiOCl and the results of these comparative studies are showed in Fig. 4. From the obtained degradation curves versus time, one can see that negligible Bisphenol A could be removed for photolysis and adsorption studies, respectively after 60 min reaction. The effect of the presence of initial H_2O_2 concentration (0.3 ml) on the degradation of BPA was investigated under UV-B light illumination, and the complete degradation (%100) of BPA could be achieved in 60 min.

The improved photocatalytic activity of the binary metal oxides in the presence of H_2O_2 are referred to form the reactive radical intermediates ($^{\bullet}OH$) from the oxidants by reaction with photogenerated electrons[26].

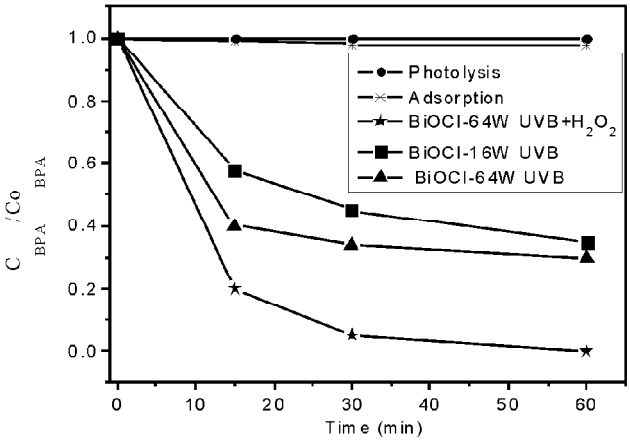

Fig. 4. Time course of the degradation of BPA.

According to a heterogeneous photocatalytic reaction process, the photocatalytic degradation rate of BPA at liquid-solid interface can be defined by the Langmuir-Hinshelwood kinetic model (eq. (4))[27]:

$$r_0 = \frac{dC}{dt} = \frac{k_0 K_\alpha C}{1 + K_\alpha C} \quad (4)$$

where r_0 is the initial rate (mg/L.min), k_r is the intrinsic rate constant (mg/L.min), K_α represents the Langmuir adsorption constant (L/mg) and C is the concentration of BPA (mg/L). The relationship can be adapted pretty well with Langmuir-Hinshelwood kinetics, demonstrating that the photocatalytic degradation of BPA by the binary metal oxides is a surface-mediated catalytic reaction. As shown in Table 1, the k_r value for BPA degradation with H_2O_2 addition and under UV-B illumination by BiOCl reaches the highest value (0.19 mg/L.min).

Table 1. Bisphenol A (BPA) degradation efficiency over 60 min (%)

Catalyst	BPA degradation efficiencies over 60 min (%)	k_r (mg/L.min)
BiOCl (16 W UVB)	65	0.012
BiOCl (64 W UVB)	70	0.016
BiOCl (64 W UVB + H_2O_2)	100	0.19

Conclusions

In the XRD of the synthesized pure crystalline BiOCl nanocomposite, all peaks shows characteristic intensity for tetragonal bismuth oxychloride and which was in good agreement with previous studies. Although there are some negli-

gible particle sizes in the SEM images, nonetheless, the SEM images and the FT-IR bands just like XRD peaks also confirms the morphological structure and the bands respectively of BiOCl nanocomposite.

It is clearly concluded that the synthesized pure BiOCl showed a good photocatalytic activity under UV-Vis light irradiation. BPA degradation was completed in 60 min. This high activity of BiOCl could be attributed to be formed Bi-O and Bi-Cl bonds at the interface as a result of chemical interaction.

Acknowledgements

This work was supported by the Scientific Research Projects Coordination Unit of the Istanbul University-Cerrahpasa (Project No. FHZ-2017-26169).

References

1. J. Yuan, J. Wang, Y. She, J. Hu, P. Tao, F. Lv, Z. Lu and Y. Gu, *J. Power Source*, 2014, **263**, 37.
2. X. Zhao, Z. Zhao, D. Wang and M. Fichtner, *Angew. Chem. Int. Ed.,* 2013, **52**, 13621.
3. J. Li, Y. Yuab and L. Zhang, *Nanoscale*, 2014, **6**, 8473.
4. F. Chen, H. Liu, S. Bagwasi, X. Shen and J. Zhang, *J. Photochem. Photobi*ol. *A*, 2010, **215**, 76.
5. L. Zhang, W. Wang, D. Jiang, E. Gao and S. Sun, *Nano Res*., 2015, **8**, 821.
6. F. M. Ascencio-Aguirre, L.Bazán-Díaz, R. Mendoza-Cruz, M. Santana Vázquez, O. Ovalle, A. Gómez-Rodríguez and R. Herrera-Becerra, *Appl. Phys. A*, 2017, **123(3)**, 1.
7. D. K. Li, L. Z. Pei, Y. Yang, Y. Q. Pei, Y. K. Xie and Q. F. Zhang, *e-J. Surf. Sci. Nanotech.,* 2012, **10(6)**,161.
8. H. L. Peng, C. K. Chan, S. Meister, X. F. Zhang and Y. Cui, *Chem. Mater.,* 2009, **21**, 247.
9. L. Y. Zhu, Y. Xie, X. W. Zheng, X. Yin and X. B. Tian, *Inorg. Chem.,* 2005, **44**, 8503.
10. P. Jagdalea, M. Castellinob, F. Marrecc, S. E. Rodil and A. Tagliaferro, *Appl. Surf. Sci.,* 2014, **303**, 250.
11. M. Gao, D. Zhang, X. Pu, M. Li, Y. Moon, J. Jeong, P. Cai, S. Kim and H. Jin, *J. Am. Ceram. Soc.,* 2015, **98**, 1515.
12. B. Sarwan, B. Pare and A. D. Acharya, *Mater. Sci. Semicond. Process*., 2014, **25**, 89.
13. X. Du, W. Zhao, Y. Liu, X. Huang and F. Mao, *Adv. Mater. Res.,* 2012, **487**, 841.
14. A. Tadjarodi, O. Akhavan, K. Bijanzad and M. M. Khiavi, *Monatsh Chem.*, 2016, **147**, 685.
15. X. Zhang, X. Wang, L. Wang, W. Kang, L. Long, W. Li and H. Yu, *Appl. Mater. Interfaces,* 2014, **6**, 7766.
16. J. Cheng, C. Wang, Y. Cui, Y. Sun and Y. Zuo, *J. Mater. Sci. Technol*., 2014, **30**, 1130.
17. Y. Li, J. Liu, J. J. Jiang and H. Yu, *Dalton Trans.,* 2011, **40**, 6632.
18. X. Hu, Y. Xu, H. Zhu, F. Hua and S. Zhu, *Mat. Sci. Semicon. Proc.,* 2016, **41**, 12.
19. S. Cao, C. Guo, Y. Lv, Y. Guo and Q. Liu, *Nanotechnology*, 2009, **20**, 275702.
20. Z. Cui, L. Mi and D. Zeng, *J. Alloys Compd.,* 2013, **549**, 70.
21. L. Cao, F. J. Spiess, A. Huang and S. L. Suib, *J. Phys. Chem. B*, 1999, **103**, 2912.
22. J. G. Hengstler, H. Foth., T. Gebel, P. J. Kramer, W. Lilienblum, H. Schweinfurth, W. Volkel, K. M. Wollin and U. Gundert-Remy, *Critic. Rev. Toxic*., 2011, **41**, 263.
23. Y. Dong, D. Y. Wu, X. C. Chen and Y. Lin, *J. Colloid Int. Sci.,* 2010, **348**, 585.
24. H. Katsumata, M. Taniguchi, S. Kaneco and T. Suzuki, *Catal. Commun*., 2013, **34**, 30.
25. Y. T. Xie, H. B. Li, L. Wang, Q. Liu, Y. Shi, H. Y. Zheng, M. Zhang, Y. T. Wu and B. Lu, *Water Res*., 2011, **45**, 1189.
26. W. F. Yao, X. H. Xu, H. Wang, J. T. Zhou, X. N. Yang, Y. Zhang, S. X. Shang and B. B. Huang, *App. Cat. B: Env*., 2004, **52**, 109.
27. Y. Xu and C. H. Langford, *J. Photochem. Photobiol. A: Chem*., 2000, **133**, 67.